

Preliminary Draft

A Comparison of Force Sensors

Richard M. Voyles, Jr.

J. Dan Morrow

Pradeep K. Khosla

Carnegie Mellon University

Advanced Manipulators Laboratory, The Robotics Institute
Carnegie Mellon University
5000 Forbes Avenue
Pittsburgh, PA 15213

July 20, 1994

© 1994 Carnegie Mellon University

The opinions represented in this report are those of the authors and do not represent the opinions of Carnegie Mellon University, The Robotics Institute, The Department of Robotics, the Department of Electrical and Computer Engineering, or any sponsoring agency. The opinions and data presented here are limited in scope and are not intended to be complete or comprehensive and are provided with no guarantee of accuracy.

1 Introduction

This report presents data gathered for evaluating 6-degree-of-freedom force/torque sensors from various manufacturers.

We set out to investigate silicon strain gage-based force sensors from Assurance Technologies, Inc. and California Cybernetics Corporation, using the old foil strain gage-based Lord Corporation sensor as a basis for comparison. We also performed a reduced set of tests on a JR³ sensor which is foil-based. The Belgian Academy of Sciences also produces 6-axis force/torque sensors but their high-speed product was not available at the time of our investigation.

“ATI” refers to Assurance Technologies, Inc., which took over the force sensor business of the Lord Corporation. ATI redesigned both the electronics and the mechanicals of the sensor to produce a radically different product. “Lord” refers to the product distributed by the Lord Corporation before the business was sold to ATI. “CCC” refers to California Cybernetics Corporation, which is a young company producing a new force sensor of its own design. “JR3” refers to JR³, Inc., which is an established company in the force sensor/load cell market.

2 Force Sensors

2.1 ATI

The ATI sensor we tested was a model 15/50. This means it is an English-units model with maximum force load of approximately 15 pounds and maximum torque load of 50 inch-pounds. The specifications claim a maximum resolved force/torque update rate of 1066 Hz with all options enabled. (We did not test data rate.) This rate can be increased to 1285 Hz by disabling several error checking and other options. It is important to note, however, that low pass filters on the strain gages have a -3dB point at 235 Hz, limiting bandwidth.

The thing that most sets this sensor apart from the CCC sensor is its three-beam design. There are 3 sense beams arranged in a “Y” configuration spaced equally at 120-degrees. Therefore, when outputting raw strain gage values, there are only 6 measurements.

This sensor weighed in at 284.72 grams (0.63 lbs) with the right angle cable attached. (Not including the weight of the cable itself.)

2.2 CCC

At this time, CCC has only one sensor model, although they claim variations are under development. (Different mechanical stiffnesses and one with off-board electronics.) This sensor is a 4-beam design (standard maltese cross) with all signal conditioning and conversion electronics on-board. (External to the sensor is the power supply and optional CPU.) The sensor provides raw strain gage data over a fiber optic link. Our test configuration included the optional VME-based 68020 single-board computer with California Cybernetics’ fiber optic interface and monitoring software. The CCC sensor is rated for a maximum force of 100 pounds and maximum torque of 60 inch-pounds.

Unique features of the CCC sensor include electronic trimming of the strain gage wheatstone half-bridges; selectable, pulsed strain gage excitation voltage; and tuned half-bridges that have matched gains. The electronic trimming of the bridges is accomplished by dedicated D/A converters on each bridge. These allow the bridges to be zeroed on command, providing full dynamic range under any arbitrary constant load. The selectable excitation feature allows user-selectable gain and increased sensitivity. The sensor beams are stiff compared to other sensors (such as the ATI 15/50), but the pulsed excitation permits higher excitation volt-

ages to achieve greater sensitivity, while the variable gain provides maximum force readings anywhere from 5 to 100 pounds. The tuned half-bridges are supposed to allow the use of a sparse calibration matrix of only ones and zeros, but the validity of this approach is somewhat suspect.

The sensor provides 63 different gain settings that varied nonlinearly over a range of about 8-to-1. We chose three different gains for comparison with the ATI sensor because no single range provided an exact match. The ATI sensor is scaled such that the ratio of torque in inch-pounds to force in pounds is roughly 3-to-1. The CCC sensor is scaled so that the equivalent ratio is roughly 1-to-1. The maximum range of each resolved component is listed in table 1 for the gains settings we used. A gain setting of 2 matched the ATI torque range around the Z axis. A gain setting of 7 approximately matched the ATI force range in X and Y. The 12 gain setting was a compromise between the X-Y and Z force ranges. It is important to note that the

Table 1: CCC Maximum Forces and Torques versus Gain Setting

Gain	X max F (lbs)	Y max F (lbs)	Z max F (lbs)	Pitch T (in-lbs)	Yaw T (in-lbs)	Roll T (in-lbs)
2	32.94	33.33	64.81	35.78	36.21	53.72
7	14.55	14.73	28.64	15.81	16.00	23.74
12	11.07	11.21	21.79	12.03	12.17	18.06

forces and torques acting on X and Y are resolved into 4095 steps (12 bits) while Z is 8191 (13 bits) on the CCC sensor. (ATI uses 12 bits on all axes.) Note that increasing gain numbers lead to increasing sensitivity.

This sensor tipped the scales at 596.90 grams (1.31 lbs).

2.3 Lord

2.4 JR3

Unlike the ATI and CCC sensors which were new evaluation units provided by the respective companies, the JR3 unit we tested was older and had been in service for some time. As such, it did not benefit from a recent calibration, as did the others. In fact, we have reason to believe that two of the strain gages were faulty. As such, we feel the noise and drift data are probably reasonable, but the cross-coupling and linearity results are suspect.

3 Total Sensor Mass

The total mass of the end-of-arm component of the sensor system is important because it impacts the maximum payload of the robot. Total end-of-arm mass appears in table 1.

Table 1: Total End-of-Arm Sensor Mass

Sensor	Mass (g)	Weight (lbs)
ATI	284.72	0.63
CCC	596.90	1.31
Lord		
JR3		

4 Noise and Drift

The drift of the sensor was monitored by gathering data for a long period of time after powering up from a thoroughly “cold” state. (i.e. the sensor was left off for at least 24 hours before running the test.) The distinction between mounting the sensor on a PUMA robot and testing it on the bench was made solely with respect to the CCC sensor because of its relatively high heat dissipation. The maximum external case temperature of the unmounted sensors in an ambient temperature of 23 degrees Celsius is shown in table 2. The

Table 2: Case Temperature for 23 C Ambient

Sensor	Temp (Celsius)
ATI	28
CCC	37
Lord	
JR3	

PUMA robot acts as a large heat sink which affects the apparent drift in the resolved force readings as shown in figures 1-5. The CCC data is broken into two plots showing the first hour and then the second hour after power up. The sensor was re-zeroed after the first hour to get a better look at the drift. Figures 3 and 4 show roughly the same drift in Newtons as figures 1 and 2 despite the lower sensitivity. (One would expect the drift, measured in bits, to remain fairly constant. Therefore, decreasing the sensitivity -- weighting each bit more heavily-- should increase the apparent drift in Newtons.) Presumably, the heat-sinking effect of the PUMA is reducing the drift commensurately. Note that the noise does increase as expected.

It is important to note that the ATI sensor (figure 6) achieves low noise primarily by filtering the signals. This low-pass filtering also limits the sensor bandwidth.

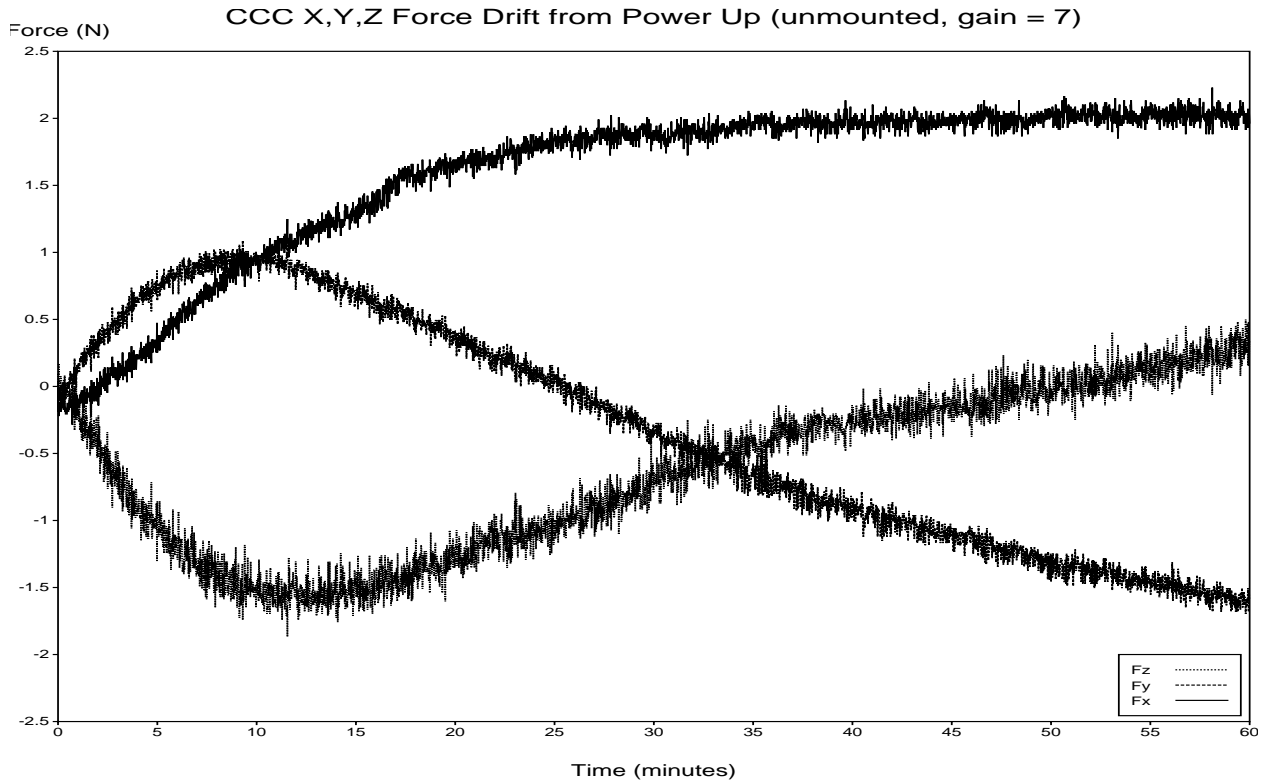


Figure 1: CCC, 1st hour after power up.

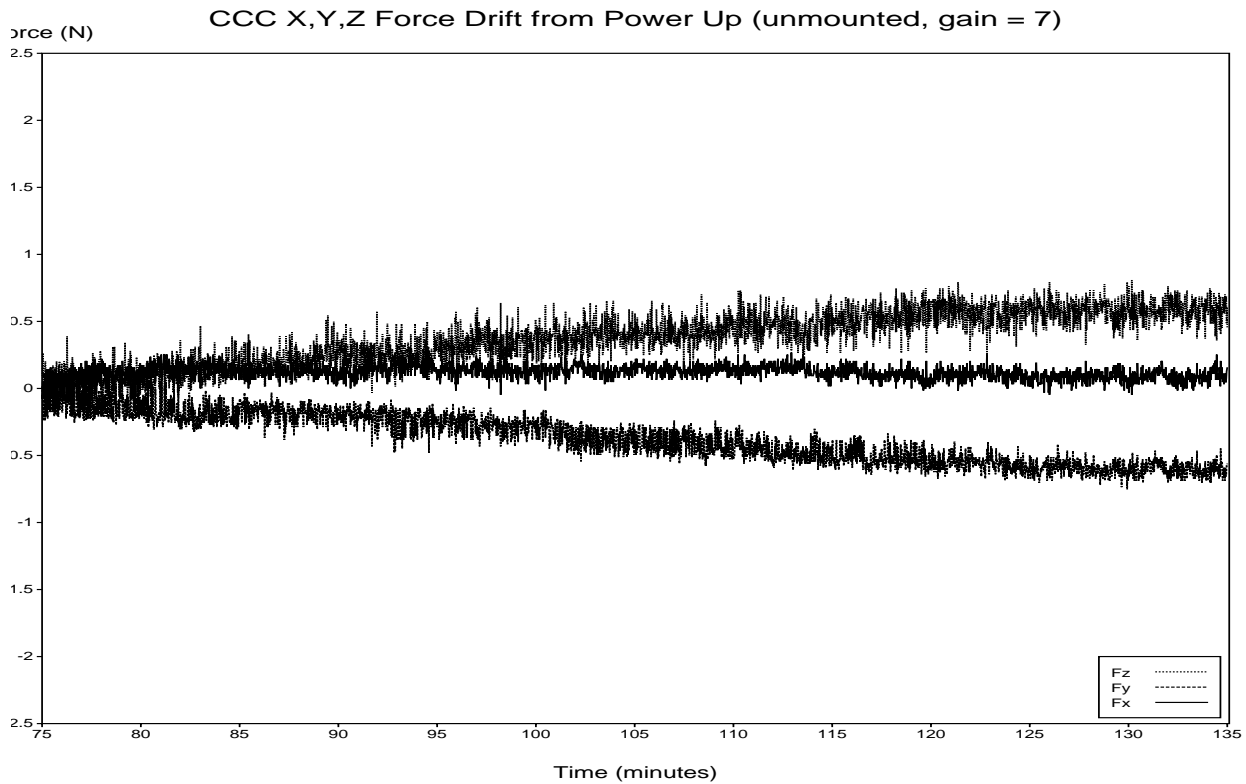


Figure 2: CCC, 2nd hour after power up.

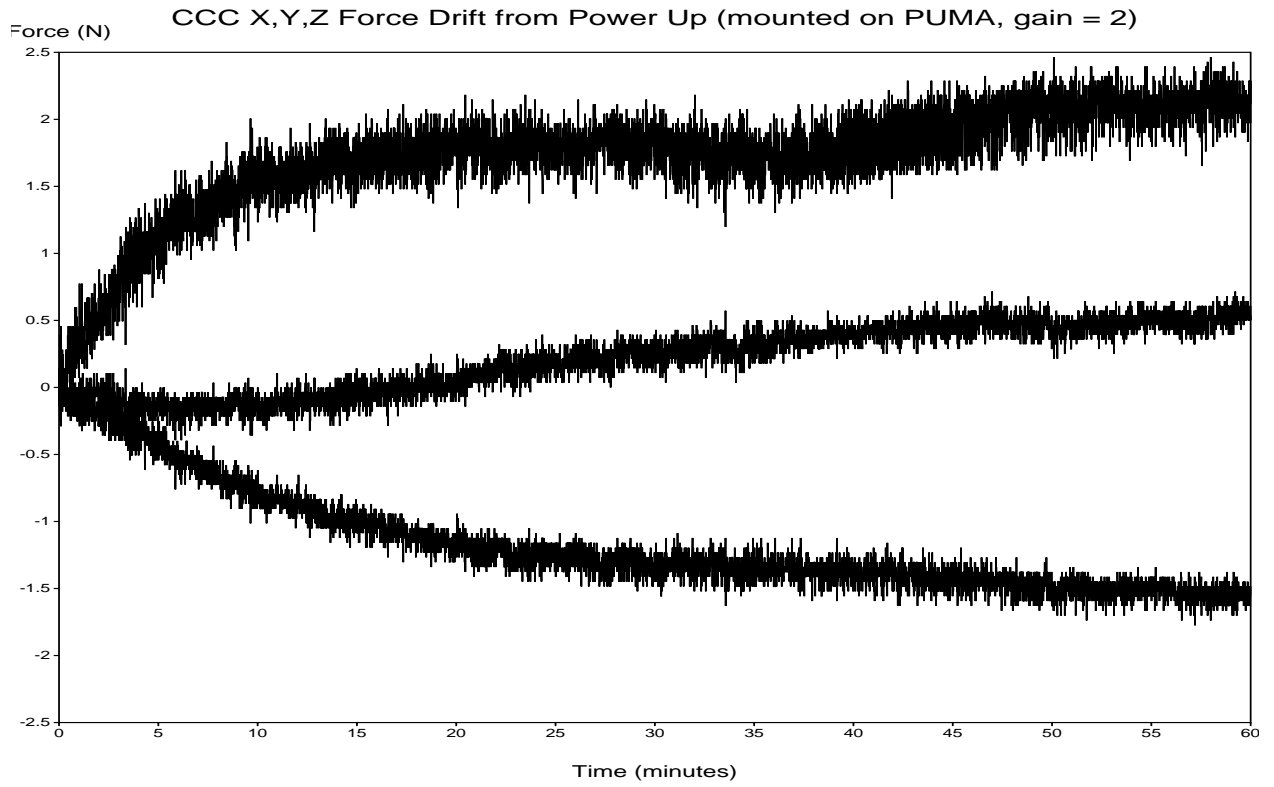


Figure 3: CCC, 1st hour mounted on PUMA

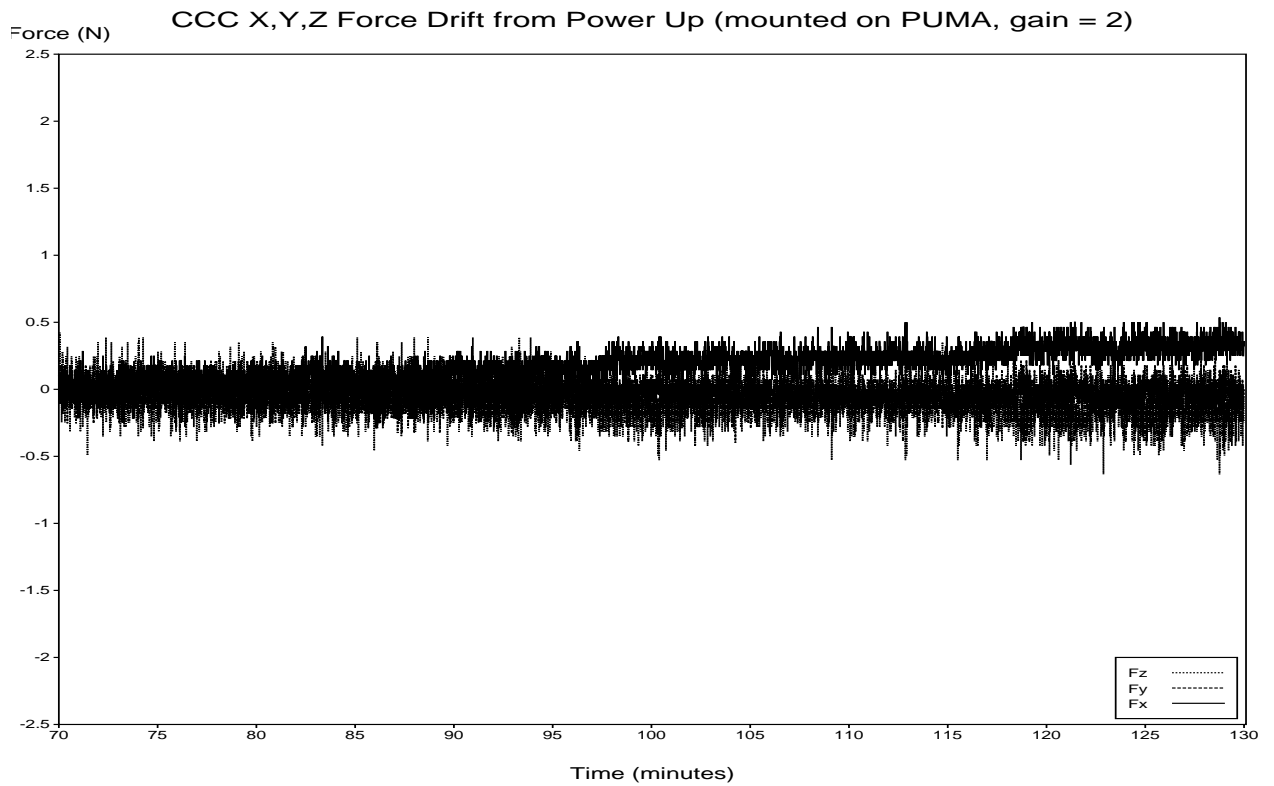


Figure 4: CCC, 2nd hour mounted on PUMA.

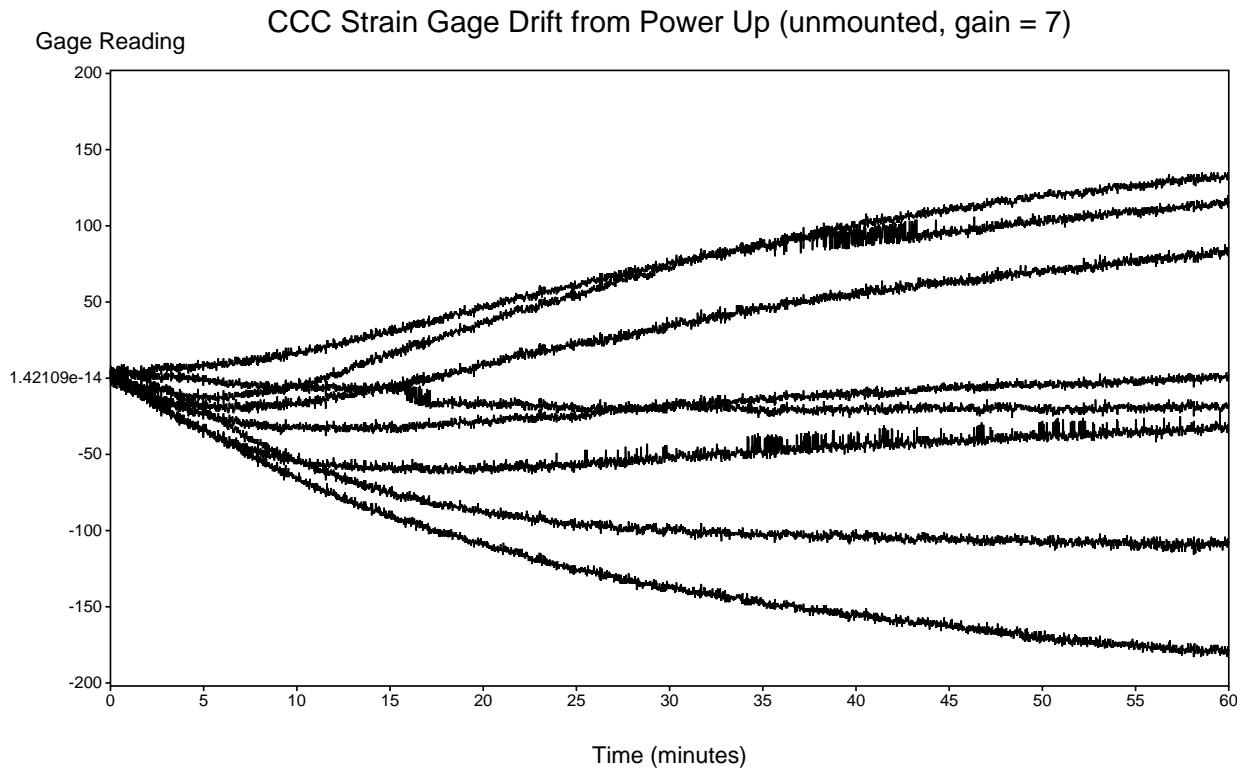


Figure 5: CCC strain gages during power up.

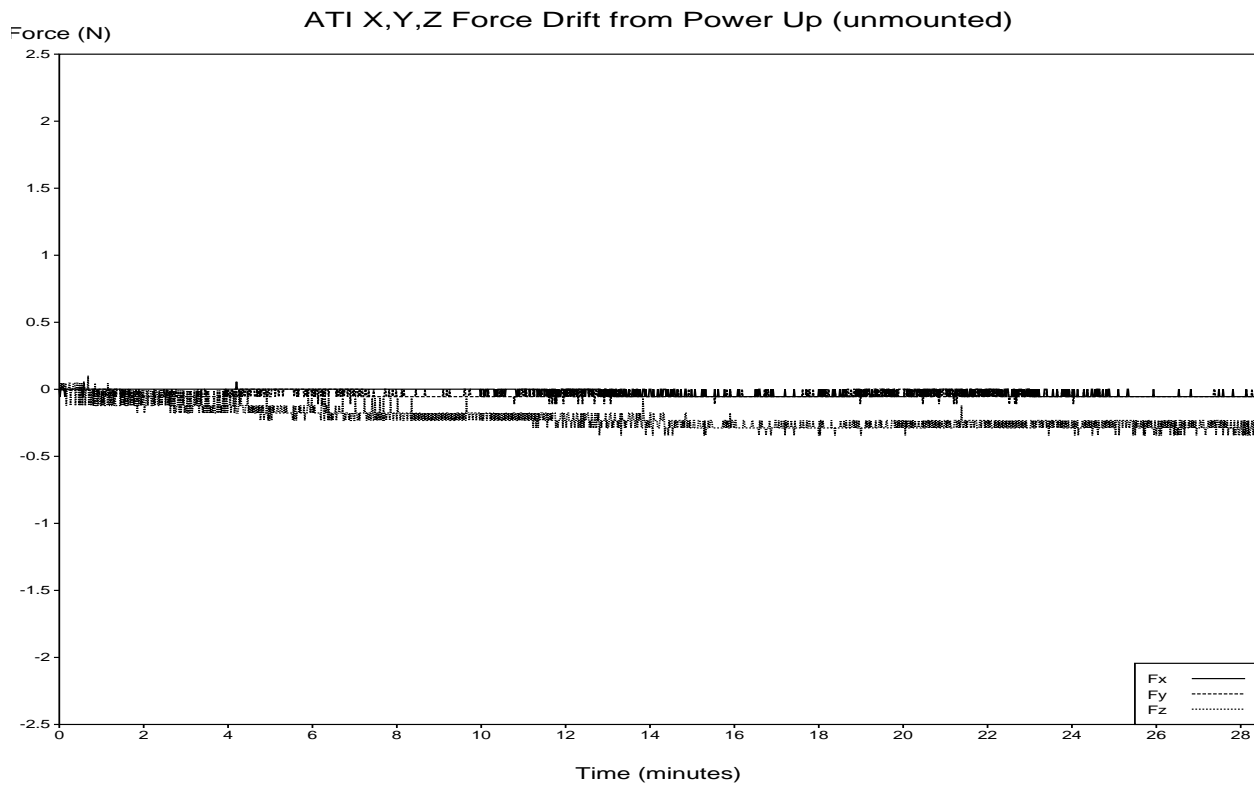


Figure 6: ATI, 1st hour after power up.

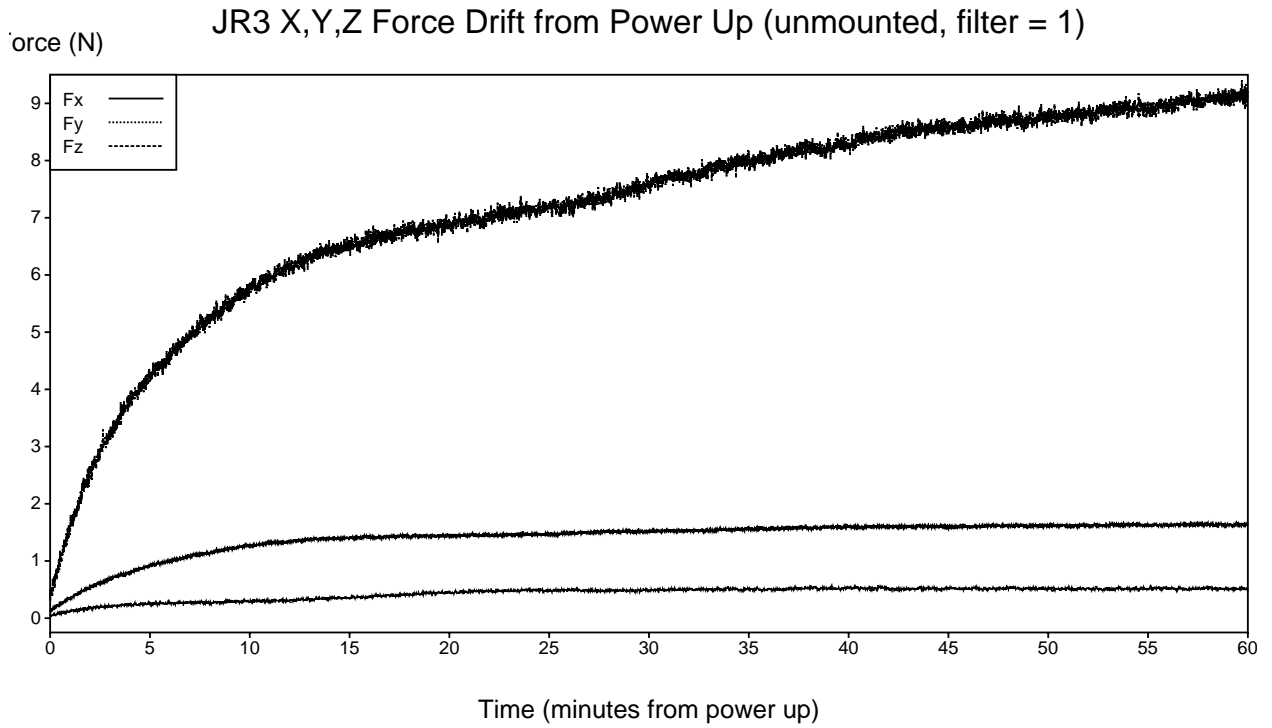


Figure 7: JR3, 1st hour from power up.

The JR3 (figures 7 & 8) was rather warm to the touch as was the CCC, but we were unable to get a case temperature measurement.

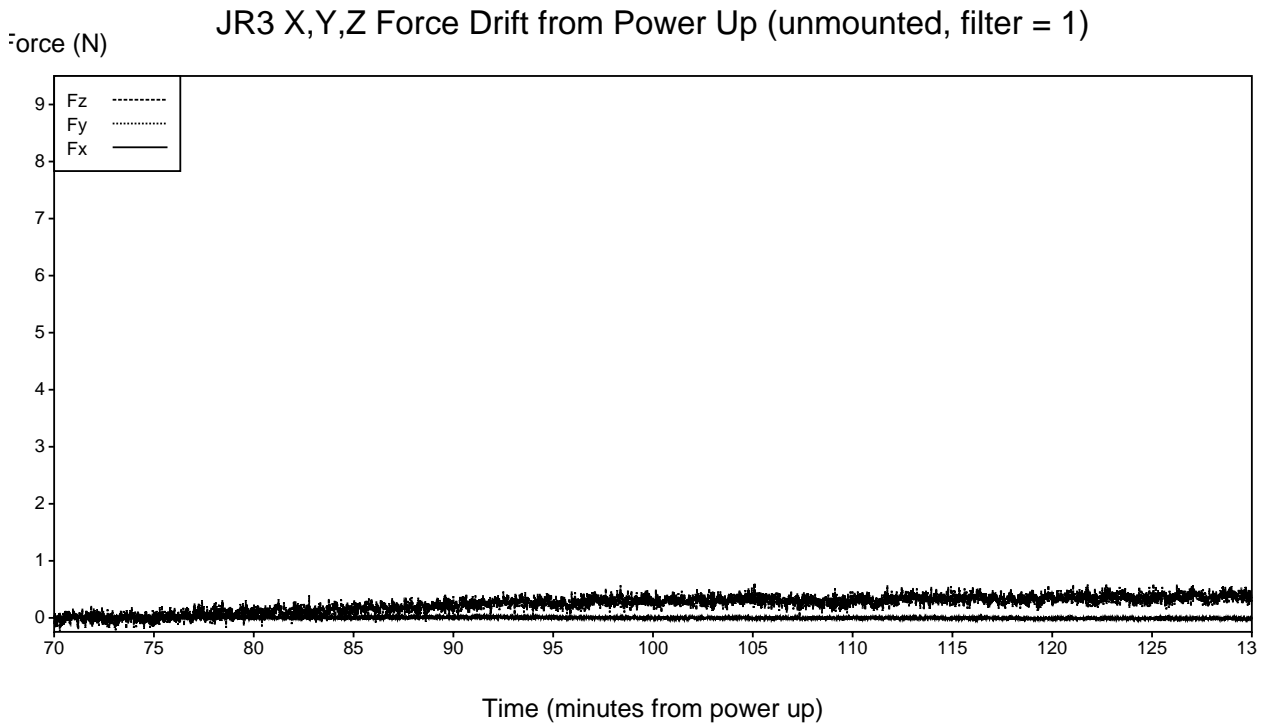


Figure 8: JR3, 2nd hour after power up.

4.1 Sensor Bandwidth

The ATI has rather aggressive filtering on each strain gage that limits the bandwidth. The 3 dB point is set by the factory to around 235 Hz. These filters are not adjustable nor can they be disabled. Additional, user selectable, sensor averaging can be performed by the sensor processor, but this is in addition to the hardware filters on-board the sensor body.

The CCC, on the other hand, has no internal filters to limit the bandwidth. California Cybernetics claims the converters can sample all eight channels up to 5000 Hz, but we did not test this aspect nor did we test the true bandwidth of the sensor. Likewise, the JR3 sensor has no hardware filters but does provide user-selectable filtering on the VME processor card. JR3 claims its sensor can sample all channels up to 8000 Hz.

5 Internal Sensor Mass

To provide a true zero, it is necessary to measure the equivalent weight of the sensing elements. To do this, we used the sensor itself and measured the apparent force of the unloaded sensor with the Z-axis pointing up and down. Half of the difference between these two readings is the true offset value and is tabulated in table 3.

Table 3: Internal Weight

Sensor	Weight (N)
CCC	1.35
ATI	
Lord	
JR3	0.55

6 Cross-Coupling

Cross-coupling refers to the erroneous measurement along some particular axis as a result of an actual force or torque applied to an orthogonal axis. Ideally, all six resolved force/torque measurements should be fully decoupled so that, for example, a pure torque applied around the X-axis does not cause the indication of a force in the Z-axis.

Since it is difficult to exert exact torques, we devised two simple experiments to measure the effects of changes in torques. In the first experiment, the sensor was attached to the PUMA robot, allowed to warm up for more than two hours, and then placed in a roughly horizontal orientation. (The Z-axis was horizontal.) A thin, stiff rod was firmly attached to the face of the force sensor and a mass was hung from the rod by a string. Sliding the fixed mass along the rod, which coincided with the Z-axis quite well, provided a varying torque while keeping the net force constant.

The second cross coupling test consisted of connecting a complex mass distribution to the force sensor in the vertical orientation and then rotating the sensor to a horizontal orientation in several increments and back to vertical again. As in experiment 1, the total force magnitude should remain constant.

6.1 CCC Cross Coupling

The data from this test on the CCC sensor is shown in figure 10. (All cross coupling measurements were performed with a gain setting of 2.) The data is inconveniently plotted versus time, but the presentation is clear enough for evaluation purposes. Each spike in the data represents a point in time at which we moved

the hanging mass along the rod. For the CCC data in figure 10, a 698-gram mass was hung about 0.5 cm

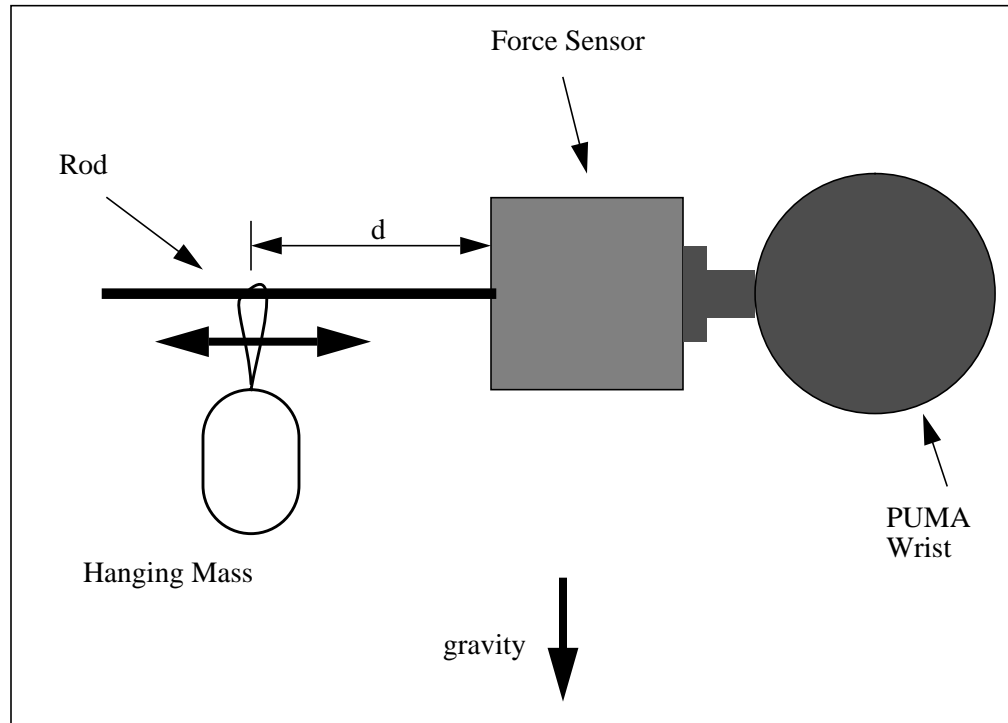


Figure 9: Diagram of the first cross-coupling test.

from the mounting face at approximately $t = 22$ seconds. It was moved in four more increments until the maximum distance, d , from the face plate was 7.5 cm which corresponded to $t = 77$ s in figure 10. The mass was then moved back in toward the face plate in three steps. The Y-axis of the sensor was not deliberately or precisely aligned with gravity but it was closest to vertical during the test. The Z axis was aligned horizontally only by “eyeballing.” so the accuracy is no more than several degrees. The important thing to note is not the absolute numbers, but the differential changes. Since the mass remains constant, neither F_y nor F_z should change. Both have noticeable slopes, however, indicating strong cross-coupling between the torque values and forces.

The surprisingly large absolute value in F_z , which should be zero, suggested the second cross coupling test. In this experiment, we connected a complex mass distribution to the force sensor in the vertical orientation and rotated the sensor to a horizontal orientation in several increments and then back to vertical. As in the first experiment, the data is plotted versus time in figure 11.

The Net Force is calculated by taking the square root of the sum of the squares of the X, Y and Z axes, but we also had to subtract out an additional bias in Z, due to the weight of the sensor beams. We determined this bias by carefully aligning the sensor face up with a level, then using the “bias” command to zero the sensor in that orientation. Then, we reoriented the sensor so it was facing straight down, again using the level. The sensor in this orientation measured a force of 2.7 N in Z. For the second cross coupling test, we subtracted one half of this amount from the Z measurements.

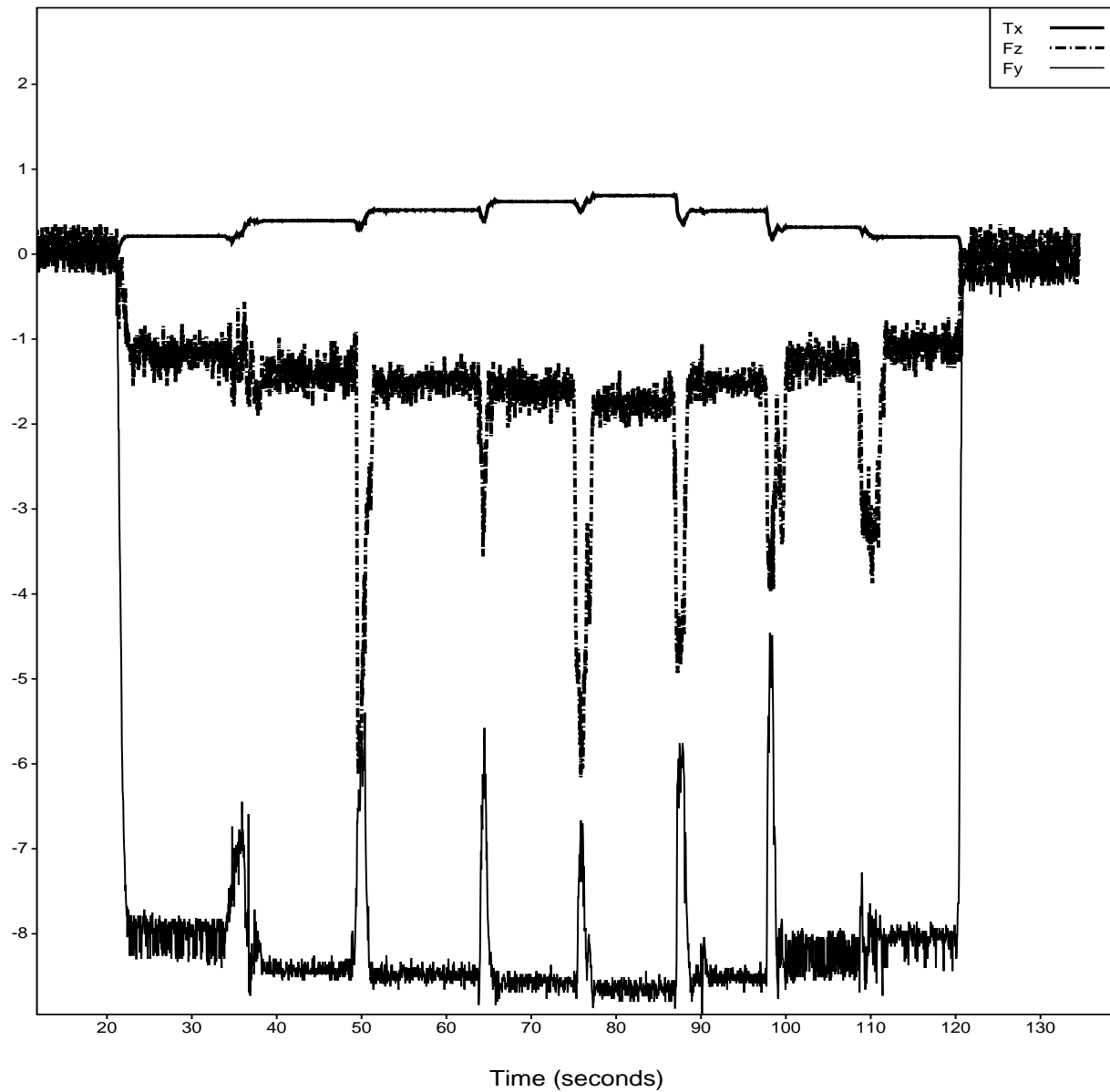
7 Linearity

To test the linearity, we oriented the sensors vertically and placed weights on the mounting plate. Measured force is the vector sum of the three force components. Data on the CCC are tabulated below in table 3 and

Table 4: CCC Linearity

Applied Mass (grams)	Measured Force (Newtons)
0.0	0.0
148.1	-1.519
371.3	-3.744

N or N-m CCC Cross Coupling (horizontal, fixed mass, varying torque)

**Figure 10: First experiment in cross coupling on the CCC.**

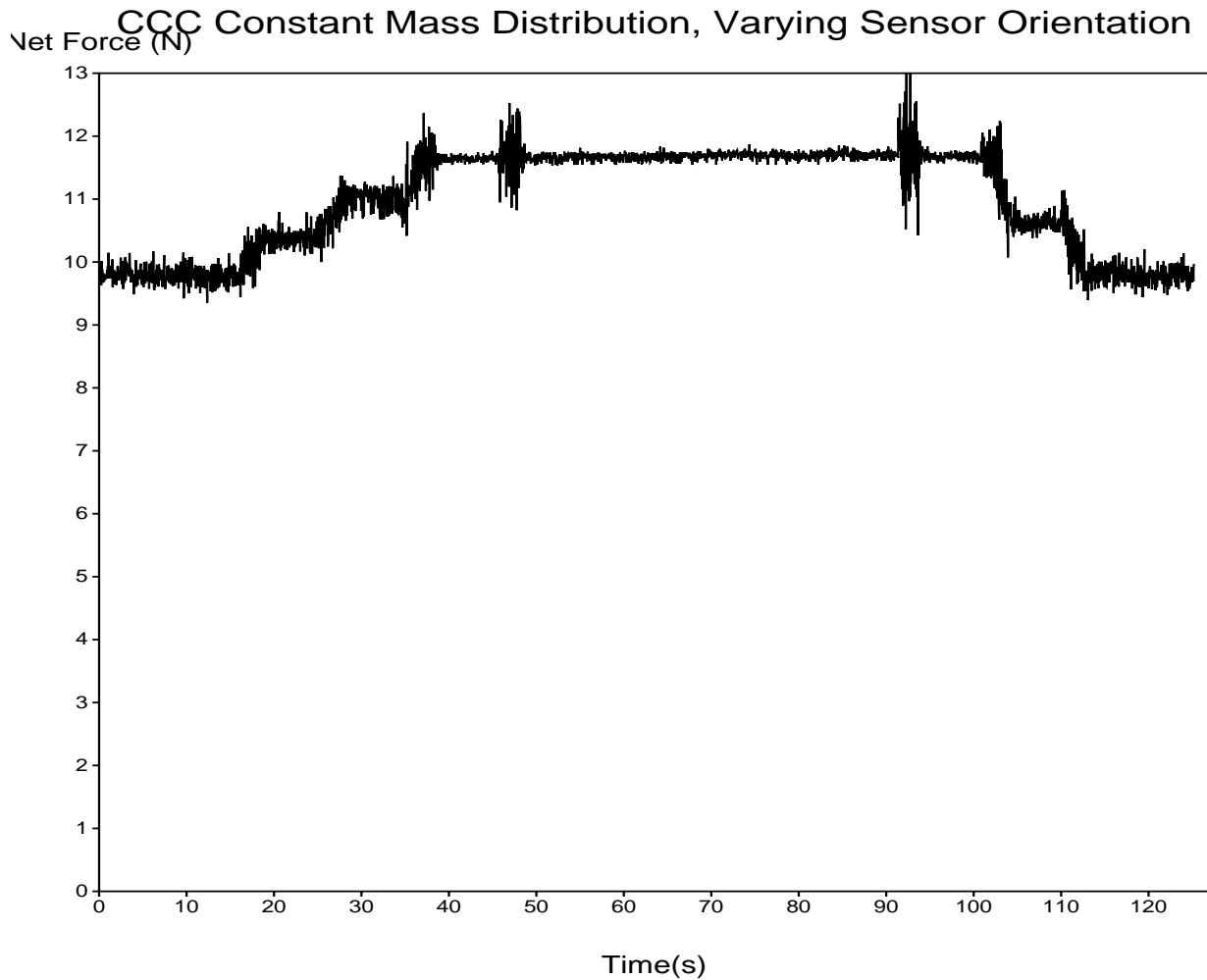


Figure 11: Second experiment in cross coupling on the CCC

Table 4: CCC Linearity

Applied Mass (grams)	Measured Force (Newtons)
743.4	-8.127

plotted in figure 12. (Conversion to N assumed $g = -9.81$.) This data is somewhat limited in usefulness due to the small excitation range relative to the maximum allowable.

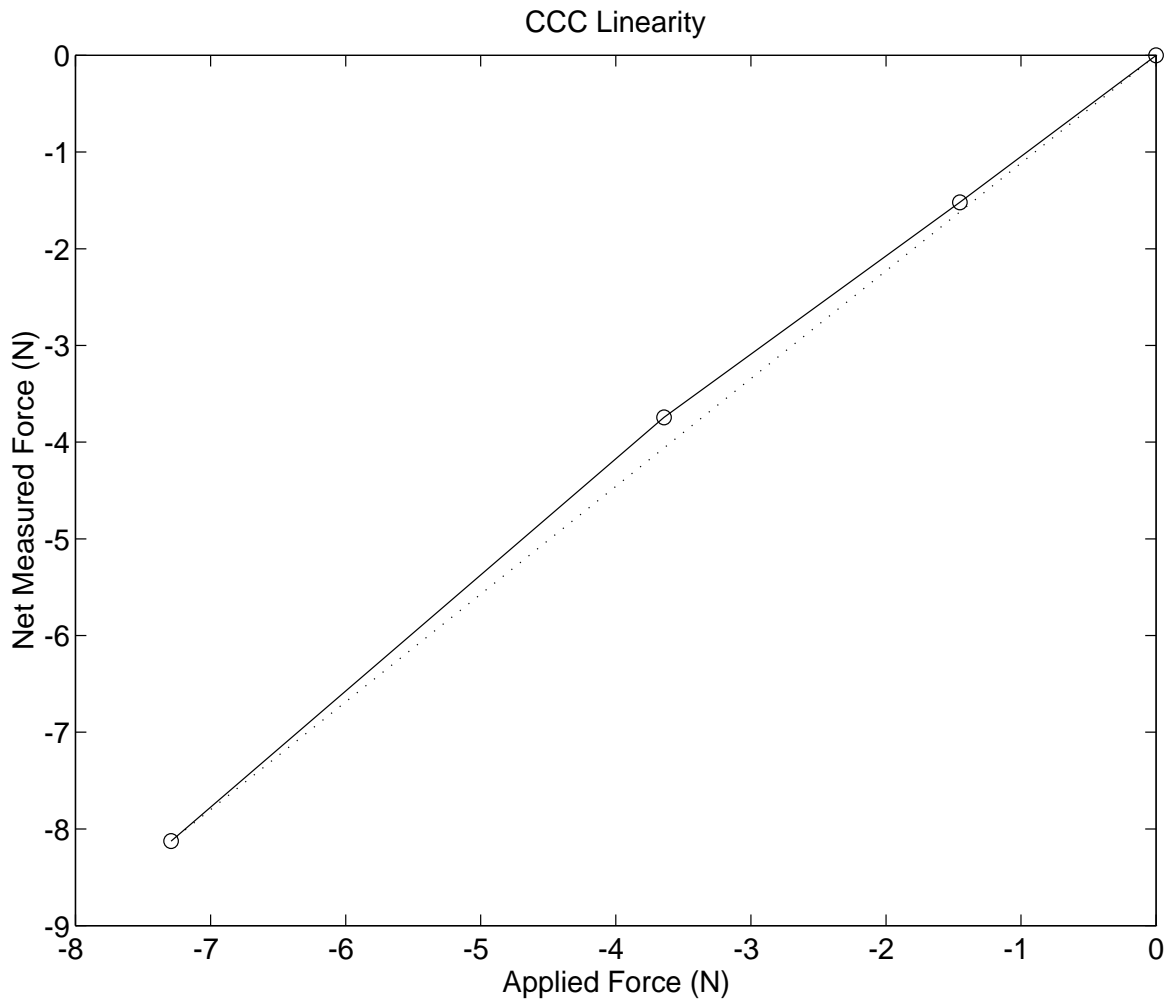


Figure 12: CCC Z-axis force linearity.